

Multi-kinks in scalar field theories with non-degenerate vacua: The commensurable and non degenerate double sine-Gordon model

Jonathan Lozano-Mayo,^a Manuel Torres-Labansat,^{b,1}

^a*Weinberg Institute for Theoretical Physics, Department of Physics, The University of Texas at Austin, Austin, TX 78712, USA*

^b*Instituto de Física, Universidad Nacional Autónoma de México, Apartado Postal 20-364, Ciudad de México 01000, México*

E-mail: Jonathanloz@utexas.edu, torres@fisica.unam.mx

ABSTRACT: This paper considers generic scalar fields models in one space dimension, the potentials of which have several vacuum states. It is shown that the partial breaking of the vacuum degeneracy provides a mechanism for the appearance of static multi-kinks, whenever some false vacuum states appear between two true vacuum states. A multi-kink is a stable field configuration with an internal structure, consisting of various localized energy packages with well-defined separations between them. General results for multi-kinks properties are presented. We introduce the commensurable and non degenerate double sine-Gordon model as a specific realization of this mechanism, supporting the existence of multi-kinks with an arbitrary n -number of subkinks. The multi-kinks properties are thoroughly analyzed including the novel phenomenology displayed when two of them collide.

KEYWORDS: Multi-kinks, dynamical Bogomol'nyi relation, modified sine-Gordon models

¹Corresponding author.

Contents

1	Introduction	1
2	General considerations	2
3	Multi-kinks in the thin-wall approximation	4
3.1	n kinks for $\alpha = 0$	4
3.2	A single multi-kink $\Phi_K(z)$ for $0 < \alpha \ll 1$	5
3.3	Dynamical Bogomol'nyi relation	6
3.4	Multi-kink mass	8
4	The commensurable and non degenerate double sine-Gordon model	8
4.1	n kinks $\phi_{k_i}(z)$ in the $\alpha = 0$ degenerate regime	9
4.2	Multi-kink Φ_K in the $\alpha > 0$ non-degenerate regime	10
4.2.1	Multi-kink mass $M_{K(n,\alpha)}$	11
4.2.2	Multi-kink profile $\Phi_K^n(z)$ and size σ_K	13
4.3	Multi-kink collisions	15
5	Conclusions	20

1 Introduction

Scalar field theories play a fundamental role in the analysis of various physical phenomena. For example, they can be used to implement the spontaneous symmetry breaking, an essential ingredient in the understanding of phase transitions and the generation of masses through the Higgs mechanism. Typically, spontaneous symmetry breaking is observed varying a control parameter of the scalar potential that generates multiple degenerate minima. In some models, the variation of another control parameter induces a partial breakdown of the degeneracy of the potential minima; in this paper we analyze some consequences of these scenarios. Being non-linear, these theories frequently predicts the existence of topological solitons, which are space localized, stable and finite energy solutions [1–5]. Even for the apparently simple case of the ϕ^4 model in one space dimension with a potential with two degenerate minima, the kinks solutions generates a rich and diverse phenomenology that is a subject of current interest [6, 7]. One aspect of particular interest is the study of the kink-antikink collisions, that for small incident velocities, concurs in a capture into a bound state, commonly referred as bion [8]. The collisions also lead to inelastic reflections in which the solitons escape to infinity after several bounces; the associated outgoing versus incident velocities plot presents a pattern of dispersion windows with an intricate chaotic behavior [9–12]. A qualitative explanation of the multi-bounces relies in the reduction of

the field degrees of freedom into a model based on a few collective coordinates: the center soliton position and the vibrational or shape modes of each kink. Hence, the bounces occur due to the reversible exchange of energy between the vibrational and translational modes [13–16].

Another paradigmatic example of one-space dimensional solitons appears in the sine-Gordon (SG) model [17, 18]. Being a completely integrable model enables obtaining exact solutions through the inverse scattering transformation method [19, 20, 22]. The solutions include not only static kink solutions, but also a rich plethora of other exact solutions like the breathers and time dependent multi-solitons in which the incidents solitons pass through each other with only a phase shift. Various extensions of the original SG model have been studied which are no longer completely integrable yet they retain some of the distinctive characteristics of the SG model [21, 35].

In recent years the exploration of scalar field models with multiple degenerate minima has been intense. The ϕ^6 model has been studied in detail, including the analysis of the kink-antikink phenomenology [23–26]. Other of these models become relevant because they allow modeling phase transitions of first and second order [27], and also to analyze the long-range non-exponential interaction between kinks [28–31].

Some of the aforementioned models incorporate multi-kink solutions with an internal structure [24, 32–35]. The goal of this paper is to show that the emergence of a multi-kink can be associated to the partial breakdown of the vacuum energy degeneracy.

Section 2 of this paper presents a general review of the kinks formalism in scalar field theories in one space dimension and the general properties of the potentials that will be considered. In section 3 we show that in general, the breaking of the potential degeneracy leads to the emergence of a static multi-kink and we also deduce a dynamical version of the Bogomol’nyi relation that allows us to determine some of the multi-kink properties. Section 4 deals with the description of the commensurable and non degenerate double sine-Gordon model, and a detailed study of the subkink solutions obtained in the degenerate limit as well as the corresponding multi-kink that emerge in the non-degenerate phase. In this section we also discuss the novel phenomenology displayed when these multi-kinks collide. The final considerations are presented in section 5.

2 General considerations

Our aim is to analyze scalar field theories in one space dimension with a generic potential $V_{n,\alpha}(\phi)$ which has $n + 1$ isolated potential minima v_i . In general we shall consider Z_2 symmetric potentials under the $\phi \rightarrow -\phi$ reflection. We denote the set of potential minima as $\mathcal{V}_{min} = \{v_i, i = \pm(0, \dots, \frac{n}{2})\}$, such that $V'_{n,\alpha}(v_i) = 0$ and $V''_{n,\alpha}(v_i) > 0$. In the considered models when $\alpha = 0$ all the minima are degenerate, and constitute the vacuum set $\mathcal{V}_0 = \{v_i\}$ with $V_{n,0}(v_i) = 0$. According to well known properties [1–5], it follows that the potential $V_{n,0}(\phi)$ supports the existence of n -kink solutions $\phi_{k_i}(z)$, where each kink interpolates between the contiguous v_{i-1} and v_i absolute potential minima, and it is characterized by a topological charge $q_i = C(v_i - v_{i-1})$, where C is an arbitrary constant. A $\alpha > 0$ value, on the other hands, breaks the potential minima degeneracy in such a way that $v_{-\frac{n}{2}}$ and

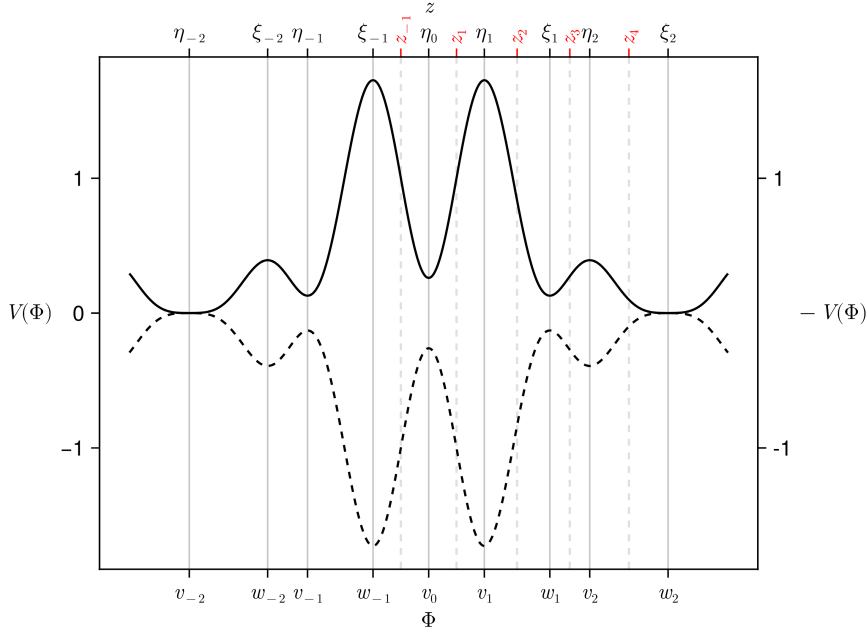


Figure 1. Potential $V_{n,\alpha}(\phi)$ (solid line) Eq.(4.1) and effective potential $-V_{n,\alpha}(\phi)$ for the classical mechanics analogy (dotted line). The parameters are selected as $n = 4$, $\alpha = 0.3$. The field values v_i and w_i correspond to the potential minima and maxima, respectively. ξ_i and η_i point out the spatial localization at which the multi-kink attains the extrema values: $V_{n,\alpha}(\Phi_K(\eta_i)) = v_i$ and $V_{n,\alpha}(\Phi_K(\xi_i)) = w_i$.

$v_{\pm \frac{n}{2}}$ remain as global minima hence $\tilde{\mathcal{V}}_0 = \{v_{-\frac{n}{2}}, v_{\frac{n}{2}}\}$ with $V_{n,\alpha}(v_{\pm \frac{n}{2}}) = 0$, but all the other intermediate minima become false vacuum states, $V_{n,\alpha}(v_i) > 0$, $i \neq \pm \frac{n}{2}$. Based on a thin-wall approximation [36], valid for small α , we will prove, that the breaking of the vacuum degeneracy induces the merging of the n kinks $\phi_{k_i}(z)$ into a single $\Phi_K(z)$ multi-kink configuration. The multi-kink possesses a topological charge given as $Q_n = \sum_i q_i$ and a mass $M_{K(n,\alpha)}$ whose approximated value will be estimated by the expression in Eq.(3.9).

The Lagrangian density for the scalar field $\phi(t, z)$ is

$$\mathcal{L} = \frac{1}{2} \left(\frac{\partial \phi}{\partial t} \right)^2 - \frac{1}{2} \left(\frac{\partial \phi}{\partial z} \right)^2 - V_{n,\alpha}. \quad (2.1)$$

For future reference in this paper, it is convenient to split the potential $V_{n,\alpha}(\phi)$ as

$$V_{n,\alpha}(\phi) = V_{n,0}(\phi) + \alpha \Delta_{n,\alpha}(\phi), \quad (2.2)$$

where $V_{n,0}(\phi)$ is a potential with $n + 1$ degenerate absolute minima, whereas the extra α contribution $\alpha \Delta_{n,\alpha}(\phi) = V_{n,\alpha}(\phi) - V_{n,0}(\phi)$ breaks the degeneracy, transforming the $n - 1$ internal minima to local, we assume that $\Delta_{n,\alpha}(0)$ is finite. An example of a potential with the described characteristics is displayed in Fig. (1)

The energy functional corresponding to the Lagrangian in Eq.(2.1) is given by the following expression

$$E[\phi] = \int_{-\infty}^{\infty} \mathcal{E} dz = \int_{-\infty}^{\infty} \left(\frac{1}{2} \left(\frac{\partial \phi}{\partial t} \right)^2 + \frac{1}{2} \left(\frac{\partial \phi}{\partial z} \right)^2 + V_{n,\alpha} \right) dz, \quad (2.3)$$

whereas the field equation of motion is given as

$$\frac{\partial^2 \phi}{\partial t^2} - \frac{\partial^2 \phi}{\partial z^2} = -\frac{dV_{n,\alpha}}{d\phi}. \quad (2.4)$$

Focusing on static configurations, the previous equation becomes

$$\frac{d^2 \phi}{dz^2} = \frac{dV_{n,\alpha}}{d\phi}, \quad (2.5)$$

multiplying this equation by $d\phi/dz$ and integrating yields the first order Bogomol'nyi equation [37]

$$\frac{1}{2} \left(\frac{d\phi}{dz} \right)^2 = V_{n,\alpha}(\phi), \quad (2.6)$$

where the integration constant is selected as zero, so the kink energy obtained from Eq.(2.3) is finite. We find convenient to define the superpotential $W_{n,\alpha}(\phi)$ [38, 39] as

$$W_{n,\alpha}(\phi) = \int^{\phi} \sqrt{2V_{n,\alpha}(\phi)} d\phi, \quad (2.7)$$

this expression together with the Bogomol'nyi Eq.(2.6) imply the relation $(d\phi/dz) = (dW_{n,\alpha}/d\phi)$.

3 Multi-kinks in the thin-wall approximation

Notice that Eqs.(2.5,2.6) are equivalent to the Newton equation for a unit mass particle with null total energy and “position ϕ ”, that evolves on “time z ” in the inverted $-V_{n,\alpha}(\phi)$ potential [2], see Fig.(1). To demonstrate the existence of a static multi-kink, we shall take advantage of this analogy and the thin-wall approximation, valid for an infinitesimal small difference between the false and true vacuum energy ($0 < \alpha \ll 1$).

3.1 n kinks for $\alpha = 0$

For $\alpha = 0$ there are n kink solutions $\phi_{k_i}(z)$, $i = \pm(1, \dots, \frac{n}{2})$, that interpolate from the v_{i-1} to the v_i minima. According to the mechanical analogy $\phi_{k_i}(z)$, is associated to an equivalent particle trajectory that departs with zero initial velocity from the “position” $\phi = v_{i-1}$ at “time” $z = -\infty$ and approaches asymptotically to $\phi = v_i$ as $z \rightarrow \infty$; clearly the point $\phi = v_i$ cannot be exceeded because the particle approaches it with vanishing velocity. The mass M_{k_i} of the kink $\phi_{k_i}(z)$ is obtained using the Bogomol'nyi Eq. (2.6) and the superpotential definition Eq. (2.7) to evaluate the energy integral in Eq. (2.3). The result is given as $M_{k_i} = \int_{v_{i-1}}^{v_i} \sqrt{2V_{n,0}(\phi)} d\phi = \int_{v_{i-1}}^{v_i} dW_{n,0} = W_{n,0}(v_i) - W_{n,0}(v_{i-1})$. The

topological content of each kink configuration $\phi_{k_i}(z)$ is related to the fact that in one-space dimension there is a topological current $J_\mu = C\epsilon_{\mu\nu}\partial^\nu\phi$, where $\epsilon_{\mu\nu}$ is the two dimensional Levi-Civita symbol and C is an arbitrary constant. J_μ is automatically conserved $\partial^\mu J_\mu = 0$, and the corresponding topological charge is $q_i = \int_{-\infty}^{\infty} J_0 dz = C \int_{-\infty}^{\infty} \frac{d\phi}{dz} dz = C(v_i - v_{i-1})$. The conservation of q_i is related to the fact that the k_i kink interpolates between different contiguous potential minima, a condition that cannot be modified by a continuous change of the field $\phi_{k_i}(z)$. For the M_{k_i} and q_i expressions the index i runs as $i = (-\frac{n}{2} + 1, \dots, \frac{n}{2})$. The results for M_{k_i} and q_i are obtained without requiring an explicit expression for the kink configuration $\phi_{k_i}(z)$. Once these are known, various multi-kink configurations can be proposed, for example $\phi_{k_i}(z+a) + \phi_{k_{i+1}}(z-a)$ represent a useful ansatz for two contiguous kinks separated by a distance $2a$. However any of these configurations will be unstable due to the existence of a repulsive force that splits the kinks apart.

3.2 A single multi-kink $\Phi_K(z)$ for $0 < \alpha \ll 1$

When α increases, the minima v_i , $i = \pm(0, \dots, \frac{n}{2} - 1)$ become local, hence an equivalent particle trajectory that start at the “position” $\phi = v_{-\frac{n}{2}}$ at “time” $z = -\infty$ no longer stops at any of the intermediate “positions” $\phi = v_i$; consequently the disconnected “trajectories” merge into a single connected “trajectory” that start at $v_{-\frac{n}{2}}$ and ends at $v_{+\frac{n}{2}}$. This results in the existence of a single multi-kink $\phi_K(z)$, composed of a chain of the n subkinks $\phi_{k_i}(z)$. To estimate the multi-kink mass $M_{K(n,\alpha)}$, we notice that in the thin-wall approximation the multi-kink profile $\Phi_K(z)$ resembles a stair with sharp steps that connect the contiguous vacuum states. Small regions around each one of the steps concentrates almost the entire energy density of each ϕ_{k_i} internal kink. Furthermore, the steps are separated by large plateaus, where the energy is that of the false vacuum states. The plots in Fig.(4,a,b) exemplify a $\Phi_K(z)$ multi-kink for which this approximation is valid..

In order to compute the multi-kink mass $M_{K(n,\alpha)}$, the z -domain in the integral in Eq.(2.3) is split into the intervals $\{z_{i-1}, z_i\}$, where $i = 1, \dots, n$, with $z_n \rightarrow \infty$ and $z_0 \equiv z_{-1}$ which are identified as the same point. As shown in Fig.(1) this assignation covers the full positive z region, and the interval $\{z_{-1}, 0\}$; the rest of the contributions corresponding to the negative axis can be easily incorporated using the Z_2 potential symmetry. The intervals $I_{A_i} = (z_{2i-1}, z_{2i})$ with $i = 1, \dots, \frac{n}{2}$ contain the points ξ_i where the potential achieves maxima value, hence $\phi(\xi_i) = w_i$ with $V'_{n,\alpha}(\omega_i) = 0$, $V''_{n,\alpha}(\omega_i) < 0$. Whereas the intervals $I_{B_i} = (z_{2i}, z_{2i+1})$ with $i = 0, \dots, \frac{n}{2} - 1$ include the points η_i where the potential becomes a minima, hence $\phi(\eta_i) = v_i$.

Regarding the contributions of the I_{A_i} regions, considering that the energy density of the ϕ_i internal kink is the leading contribution, we can safely set $\alpha = 0$ and use the Bogomol'nyi Eq. (2.6) to estimate

$$\Delta M_{A_i} = \int_{z_{2i-1}}^{z_{2i}} \left(\frac{d\phi_{k_i}}{dz} \right)^2 dz \approx \int_{\eta_{i-1}}^{\eta_i} \left(\frac{d\phi_{k_i}}{dz} \right)^2 dz = \int_{v_{i-1}}^{v_i} dW_{n,0} = W_{n,0}(v_i) - W_{n,0}(v_{i-1}) = M_{k_i}. \quad (3.1)$$

The previous calculations requires extending the integration region from (z_{2i-1}, z_{2i}) to (η_{i-1}, η_i) , which is a reasonable approximation because the density energy $\left(\frac{d\phi_{k_i}}{dz} \right)^2$ is dis-

tributed in a very narrow bump, hence its integration is essentially the same in both intervals. Notice that now $\phi_{k_i}(z)$ interpolates between false instead of true vacuum states, hence by itself each internal kink would be unstable. Interestingly, the interaction with the contiguous kinks gives place to a stable multi-kink configuration.

In order to calculate the energy contribution from the I_{B_i} intervals, based on the fact that in the mechanical analogy the particle spends a long “time z ” around the region $\phi \approx v_i$, we expect the field to display a pronounced plateau. Thus in the I_{B_i} region we can approximate $\left(\frac{d\phi}{dz}\right) \approx 0$ and $V(\phi(z)) \approx V(v_i) = \alpha \Delta_{n,\alpha}(v_i)$. Hence the contribution to the multi-kink mass is estimated as

$$\Delta M_{B_i} \approx \int_{z_{2i}}^{z_{2i+1}} V_{n,\alpha}(\phi) dz \approx \int_{\xi_i}^{\xi_{i+1}} V_{n,\alpha}(v_i) dz = (\xi_{i+1} - \xi_i) \alpha \Delta_{n,\alpha}(v_i). \quad (3.2)$$

Where the thin-wall approximation justifies extending the integration region from (z_{2i}, z_{2i+1}) to (ξ_i, ξ_{i+1}) . Considering that the kink center ξ_i is identified with the point at which the potential attains its maximum value $V_{n,\alpha}(\phi(\xi_i)) = w_i$ [28], it follows that $\xi_{i+1} - \xi_i$ represents the equilibrium separation between the ϕ_{k_i} and $\phi_{k_{i+1}}$ internal kinks. In the next section we shall preset a method to determine this quantity.

3.3 Dynamical Bogomol’nyi relation

We generalize the method recently introduced by Manton [28], to obtain a dynamical Bogomol’nyi relation, that allow us to find the effective force that acts between the ϕ_{k_i} and $\phi_{k_{i+1}}$ kinks, and from that to determine their equilibrium $\xi_{i+1} - \xi_i$ separation .

We assume that the multi-kink configuration $\phi(z)$ satisfies the exact static field equation Eqs.(2.5, 2.6), except in the region $\xi_i \leq z \leq \eta_{i+1}$, where the field $\varphi(z, t)$ departs from the exact $\phi(z)$, and it is given by the $\alpha = 0$ kink $\phi_{k_{i+1}}$. Outside this region, the exact field configurations $\phi(z)$ remains intact. The modified field becomes time dependent and is centered at $z = x(t)$, thus is written as $\varphi(z - x(t))$, where $x(t)$ represents the position of the subkink k_{i+1} . At equilibrium $\varphi(z - x(t))$ is expected to relax to the exact configuration $\phi(z)$ and $x(t) \rightarrow \xi_{i+1}$. Substituting $\varphi(z - x(t))$, into the time dependent field equation Eq.(2.4) gives

$$\gamma^{-2} \frac{d^2 \varphi}{d^2 y} - \frac{dV_{n,\alpha}}{d\varphi} + \ddot{x} \frac{d\varphi}{dy} = 0, \quad (3.3)$$

where $y = z - x(t)$ is the argument of φ and $\gamma = 1/\sqrt{1 - \dot{x}^2}$ is the Lorentz contraction factor. Eq.(3.3) can be considered a quasi-static equation for the field $\varphi(y)$ that evolves adiabatically on time trough its dependence on $x(t)$. In what follows we shall assume that the acceleration \ddot{x} , and the velocity \dot{x} are small, so only leading terms in these quantities will be retained. Multiplying Eq.(3.3) by the term $d\varphi/dy$, and utilizing the relation $d\varphi/dy = dW_{n,\alpha}/d\varphi$ leads to the following expression $\frac{d}{dy} \left(\frac{1}{2} \left(\frac{\partial \varphi}{\partial y} \right)^2 - V_{n,\alpha} + \ddot{x} W_{n,\alpha} \right) = 0$, that is easily integrated from an arbitrary value of z to $z = \eta_{i+1}$, where $\varphi = v_{i+1}$, to give the following expression

$$\frac{1}{2} \left(\frac{d\varphi}{dy} \right)^2 = [V_{n,\alpha}(\varphi) - \ddot{x} (W_{n,\alpha}(\varphi) - W_{n,\alpha}(v_{i+1}))], \quad (3.4)$$

where we used the fact that φ satisfy the Bogomol'nyi relation Eq.(2.6) $\left[\frac{1}{2} \left(\frac{d\varphi}{dy} \right)^2 - V_{n,\alpha}(\varphi) \right]_{z=\eta_{i+1}} = 0$, at the boundary. Comparing with Eq.(2.6), we observe that Eq.(3.4) can be considered an adiabatic time dependent Bogomol'nyi relation, where the potential $V_{n,\alpha}(\varphi)$ is replaced by an effective potential $V_{eff} = V_{n,\alpha}(\varphi) - \ddot{x} (W_{n,\alpha}(\varphi) - W_{n,\alpha}(v_{i+1}))$.

For a given trajectory $x(t)$, the solution of Eq.(3.4) determines the adiabatic evolution of the field φ . Additionally, an integration of this equation throws an expression for the evolution of the coordinate $x(t)$. The limits are selected from $z = \xi_i$ where $\varphi = \omega_i$, to $z = x(t)$ with $\varphi(x(t)) \rightarrow \omega_{i+1}$, to obtain

$$\int_{\omega_i}^{\omega_{i+1}} \frac{d\varphi}{\sqrt{2 [V_{n,\alpha}(\varphi) + \ddot{x} (W_{n,\alpha}(v_{i+1}) - W_{n,\alpha}(\varphi))]} = x(t) - \xi_i. \quad (3.5)$$

This equation represents an implicit relation between the kink acceleration \ddot{x} and $x(t)$, that is the effective equation of motion for the coordinate $x(t)$. In particular, equilibrium is reached when $\ddot{x} \rightarrow 0$ and $x(t) \rightarrow \xi_{i+1}$, leading to the correct expression for the separation between the contiguous k_i and k_{i+1} kinks, it reads

$$\int_{\omega_i}^{\omega_{i+1}} \frac{d\varphi}{\sqrt{2 [V_{n,\alpha}(\varphi)]}} = \xi_{i+1} - \xi_i. \quad (3.6)$$

Approximated analytical expressions for the equation of motion for $x(t)$ and the equilibrium separation $\xi_{i+1} - \xi_i$ can be obtained from Eq.(3.5). The leading contribution to the integral in Eq.(3.5) arises from values of φ in the region close to the potential minimum $\varphi \sim v_i$. Hence we expand the potential $V_{n,\alpha}(\varphi) = V_{n,0}(\varphi) + \alpha \Delta_{n,\alpha}(\varphi) \approx \alpha \Delta_{n,\alpha}(v_i) + \frac{1}{2} m_i^2 (\varphi - v_i)^2$, where $m_i^2 = (d^2 V_{n,\alpha} / d^2 \varphi)_{\varphi=v_i}$ is the mass of the perturbative scalar oscillations around v_i , and we verify that to leading order $W_{n,\alpha}(\varphi) \approx W_{n,\alpha}(v_i)$. Identifying $W_{n,\alpha}(v_{i+1}) - W_{n,\alpha}(v_i) = M_{k_{i+1}}$ as the ϕ_i kink mass, the resulting expression is readily integrated and the relation between \ddot{x} and x takes the form of a Newton equation of motion,

$$M_{k_{i+1}} \ddot{x} = F(x) = 2m_i^2 [(\omega_{i+1} - v_i)(v_i - \omega_i)] e^{-2m_i(x-\xi_i)} - \alpha \Delta_{n,\alpha}(v_i). \quad (3.7)$$

The first contribution is identified with the repulsive force which usually acts between kinks, but an additional attractive term arises due to the negative pressure exercised by the false vacuum region trapped between the kinks pair. At equilibrium $x(t) \rightarrow \xi_{i+1}$, and the vanishing of the force determines the equilibrium separation as

$$\xi_{i+1} - \xi_i = \frac{1}{m_i} \ln \left[\frac{2((\omega_{i+1} - v_i)(v_i - \omega_i) m_i^2)}{\alpha \Delta_{n,\alpha}(v_i)} \right]. \quad (3.8)$$

3.4 Multi-kink mass

We now go back and put together the results of the two previous sections in order to write down the expression for the multi-kink mass $M_{K(n,\alpha)}$. The energy density of an internal kink is localized in a small region around a potential maxima, and it contributes with a term of the form $\Delta M_{A_i} \approx M_{k_i} + \mathcal{O}(\alpha)$, Eq.(3.1). On the other hand at the plateau regions around the potential minima, the contribution was estimated in Eq.(3.2) as $\Delta M_{B_i} \approx \alpha \Delta_{n,0}(v_i)(\xi_{i+1} - \xi_i)$. Putting all the terms together we finally obtain the following expression for the multi-kink mass

$$M_{K(n,\alpha)} = 2 \sum_{i=1}^{\frac{n}{2}} M_{k_i} + \sum_{i=0}^{\frac{n}{2}-1} (2 - \delta_{i,0}) \frac{\alpha \Delta_{n,0}(v_i)}{m_i} \ln \left[\frac{2 (\omega_{i+1} - v_i) (v_i - \omega_i) m_i^2}{\alpha \Delta_{n,0}(v_i)} \right]. \quad (3.9)$$

The first term results from the sum of the kinks masses that exist in the degenerate $\alpha = 0$ limit, whereas the second one arises from the $n - 1$ contiguous pairwise kink interactions evaluated at the equilibrium positions given in Eq.(3.8); the delta Kronecker term takes into account that the $\phi_{k_{-1}} - \phi_{k_1}$ interaction contributes only once. The corrections to Eq.(3.9) are of order $\mathcal{O}(\alpha)$, hence they can be neglected in the $\alpha \ll 1$ limit. The $\alpha \log(1/\alpha)$ dependence of the multi-kink mass has been previously obtained for some particular scalar field models [24, 32–34]. Our work proves it to be valid for a generic scalar potential as a result of the vacuum degeneracy breakdown.

4 The commensurable and non degenerate double sine-Gordon model

Let us now consider a double sineGordon model in which the usual SG potential $(1 - \cos \phi)$ is shifted by the breaking degeneracy parameter α and modulated by a second SG term $(1 + \cos \frac{\phi}{n})$ with $2\pi n$ periodicity. The potential takes the form

$$V_{n,\alpha}(\phi) = \frac{1}{2(1 + \frac{1}{2}|\alpha|)} (1 - \cos \phi + \alpha) \left(1 + \cos \frac{\phi}{n} \right). \quad (4.1)$$

The potential reduces to the usual SG potential when $\alpha = 0$ and $n \rightarrow \infty$, while for $\alpha \rightarrow \infty$ it also leads to a SG potential for $\phi \rightarrow \frac{\phi}{n} + \pi$. $V_{n,\alpha}$ is invariant under the $\phi \rightarrow -\phi$ and $\phi \rightarrow \phi + 2\pi n$ transformations, so unless otherwise specified we shall refer to the solutions in the $\phi \in \{-\pi n, \pi n\}$ sector. For simplicity we assume n is an even integer, similar results are obtained in the n -odd case.

The $n + 1$ potential minima can be numerically determined, however a useful approximation is worked out for small α

$$v_i \approx 2i\pi + \frac{\alpha \sin\left(\frac{2\pi i}{n}\right)}{2n \cos^2\left(\frac{\pi i}{n}\right)}, \quad i = \pm \left(0, 1, 2, \dots, \frac{n}{2} - 1\right), \quad v_{\pm \frac{n}{2}} = \pm n\pi. \quad (4.2)$$

There are $n + 1$ perturbative scalar excitations associated with these vacuum states, with masses determined from $m_i = \frac{d^2 V_{n,\alpha}(\phi)}{d^2 \phi} \Big|_{\phi=v_i}$, that are given as

$$m_i \approx \cos\left(\frac{i\pi}{n}\right) - \frac{\alpha}{4n^2} \frac{(1 + 4\sin^2(\frac{\pi i}{n}))}{\cos(\frac{i\pi}{n})}, \quad i = \pm\left(0, 1, 2, \dots, \frac{n}{2} - 1\right), \quad m_{\pm\frac{n}{2}} = \sqrt{\frac{\alpha}{2n^2}}. \quad (4.3)$$

All positive values of $\alpha \in \{0, \infty\}$ yield kink solutions. When $\alpha = 0$ the model admits n kink solutions ϕ_{k_i} . As α increases the internal kinks merge into a single Φ_K multi-kink. The internal structure of Φ_K with well defined bump energy concentrations, will be evident in the interval $0 < \alpha \leq \alpha_1$; α_1 shall be later determined in Eq.(4.18). The internal kinks will overlap increasingly in the region $\alpha_1 < \alpha \leq \alpha_2$. α_2 represents a threshold from which the local minima begin to disappear. This value is estimated as

$$\alpha_2 = \frac{n \left[1 - \cos(\frac{3\pi}{2n})\right]}{\sin(\frac{3\pi}{2n})} - 1. \quad (4.4)$$

Increasing α beyond α_2 leads to the progressive disappearance of the internal kinks, until Φ_K reduces to a single soliton with no internal structure. Although soliton solutions are not expected for negative values of α , the model admits the possibility of saddle point solutions bouncing between false and true vacuum. These solutions, known as sphalerons [39, 40], will be studied in future work.

4.1 n kinks $\phi_{k_i}(z)$ in the $\alpha = 0$ degenerate regime

For $\alpha = 0$ the potential minima are located at $v_i = 2i\pi$ with $i = \pm(0, 1, 2, \dots, \frac{n}{2})$, thus the model has n kink solutions $\phi_{k_i} \in \{v_i, v_{i+1}\}$, $i = -\frac{n}{2}, \dots, 0, \dots, \frac{n}{2}$, with the same topological charge $q_{k_i} = \frac{1}{2\pi}(v_{i+1} - v_i) = 1$ and their corresponding antikinks $\bar{\phi}_{k_i}$ with $\bar{q}_{k_i} = -1$. The location of potential maxima ω_i depart from $\omega_i = \pm(2i-1)\pi$, valid for the SG model. Their values are obtained from the solutions of the equation $n \cot(\frac{\phi}{2}) - \tan(\frac{\phi}{2n}) = 0$. Since the shifts from the $\omega_i = (2i-1)\pi$ values are in general small, a very good approximation can be obtained as

$$\omega_i \approx \left((2i-1)\pi - \frac{2n \tan\left[\frac{(2i-1)\pi}{2n}\right]}{n^2 + \sec^2\left[\frac{(2i-1)\pi}{2n}\right]} \right), \quad i = \pm\left(1, 2, \dots, \frac{n}{2}\right). \quad (4.5)$$

The superpotential, Eq.(2.7) is calculated as $W[\phi] = -\frac{4n}{n^2-1} \left(n \cos \frac{\phi}{2} \cos \frac{\phi}{2n} + \sin \frac{\phi}{2} \sin \frac{\phi}{2n} \right)$, hence the kink masses are expressed as

$$M_{k_i} = W[v_i] - W[v_{i-1}] = \frac{4n^2}{n^2-1} \left(\cos \frac{v_i}{2n} + \cos \frac{v_{i-1}}{2n} \right), \quad i = \pm\left(1, 2, \dots, \frac{n}{2}\right). \quad (4.6)$$

It is interesting to observe that, using to Eqs.(4.3,4.6), the masses M_{k_i} are related to the scalar field masses defined at the contiguous minima v_i and v_{i-1} as follows $M_{k_i} = \frac{4n^2}{n^2-1} (m_i + m_{i-1})$.

The $\phi_{k_i}(z)$ field configurations correspond to the solutions of the equation

$$\frac{d\phi}{dz} = 2 \sin \frac{\phi}{2} \cos \frac{\phi}{2n}. \quad (4.7)$$

For $n = 2$, Eq.(4.7) has the implicit analytical solution $\log \left[\tan(\frac{\phi}{8}) \right] + \sec(\frac{\phi}{4}) = z$. For any other value of n , it can be solved numerically. However, a very good analytical approximation can be obtained observing that in general the term $\cos \frac{\phi}{2n}$ varies slowly compared with $\sin \frac{\phi}{2}$ in each kink sector $\phi \in \{v_{i-1}, v_i\}$. This enables implementing an approach that will be referred to as the smooth-modulation approximation, which becomes more precise as n grows. When the slowly varying term $\cos \frac{\phi}{2n}$ is evaluated at the extreme points $\phi \sim v_{i-1}$ or $\phi \sim v_i$, the solutions of Eq.(4.7) coincide with the well known SG field solution with the asymptotic behavior $\phi(z) \sim v_{i-1} + \text{const} e^{m_{i-1}z}$ or $\phi(z) \sim v_i - \text{const} e^{-m_i z}$ as $z \rightarrow \mp\infty$. The previous results are valid, except near the absolute minima, where according to Eq.(4.3) the scalar mass $m_{\pm n/2}$ cancels, thus the correct asymptotic behavior is worked out as $\phi(z) \sim \mp n\pi \pm \frac{4n}{z}$. The above suggests an ansatz for $\phi_{k_i}(z) \in \{v_{i-1}, v_i\}$, that correctly reproduces the asymptotic behavior in each interval, given as

$$\phi_{k_i}(z) = v_{i-1} + 4 \tan^{-1} G_i[z], \quad i = 1, \dots, \frac{n}{2}, \quad (4.8)$$

$$G_i[z] = \frac{1}{a_i e^{-m_{i-1}z} + b_i e^{-m_i z}}, \quad i < \frac{n}{2}, \quad G_{\frac{n}{2}}[z] = \log \left[1 + \frac{1}{c_n e^{-m_{\frac{n}{2}-1}z} + d_n e^{-z/n}} \right].$$

The solutions for negative values of i are obtained from the previous expressions as $\phi_{k_{(-i)}}(z) = -\phi_{k_i}(-z)$, $i = 1, \dots, \frac{n}{2}$. Given that $m_{i-1} > m_i$, the $\phi_{k_i}(z)$ ansatz correctly reproduces the asymptotic exponential tails determined by the scalar masses m_{i-1} and m_i . For the function $G_{\frac{n}{2}}[z]$ in the interval $\phi \in \{v_{\frac{n}{2}-1}, v_{\frac{n}{2}}\}$, both an exponential $\phi(z) \sim (n-2)\pi + \frac{4}{c_n} e^{-m_{\frac{n}{2}-1}z}$ and a long range $\phi(z) \sim n\pi - \frac{4n}{z}$ tail behavior are reproduced. The coefficients a_i , b_i , c_n and d_n are obtained requiring that at the kink center $z = 0$ the field value coincide with the potential maxima $\phi_{k_i}(0) = \omega_i$, and the field derivative at this point is determined by Eq.(4.7). The explicit results are worked out as

$$a_i = \frac{\gamma_i \mu_i - m_i}{\gamma_i (m_{i-1} - m_i)} \quad b_i = \frac{m_{i-1} - \gamma_i \mu_i}{\gamma_i (m_{i-1} - m_i)}, \quad i = 1, \dots, \frac{n}{2} - 1, \quad (4.9)$$

where $\gamma_i = \tan \frac{\omega_i - v_{i-1}}{4}$ and $\mu_i = \sin \frac{\omega_i}{2} \cos \frac{\omega_i}{2n} / \left(2 \sin^2 \frac{(\omega_i - v_{i-1})}{4} \right)$, whereas

$$c_n = \frac{n\nu_n - \kappa_n}{n \sin \frac{\pi}{n} - 1} \quad d_n = \frac{n(\kappa_n \sin \frac{\pi}{n} - \nu_n)}{n \sin \frac{\pi}{n} - 1}, \quad (4.10)$$

with $\nu_n = \frac{\kappa_n}{4}(\kappa_n + 1)(1 + \gamma_n^2) \sin \left(\frac{\omega_{n/2}}{2} \right) \cos \left(\frac{\omega_{n/2}}{2n} \right)$, $\kappa_n = (e^{\gamma_n} - 1)^{-1}$, and $\gamma_n = \tan \frac{\omega_{n/2} - (n-2)\pi}{4}$.

Figure (2) displays the $\phi_{k_i}(z)$ kinks profiles obtained from the numerical solutions of Eq.(4.7) as compared with the analytical results of Eq.(4.8). We observe that the smooth-modulation approximation works very well, providing solutions that for $n > 2$, show an excellent coincidence with the numerical results. For ease of notation and future reference, each kink $\phi_{k_i}(z)$ will be sometimes denoted as k_i , and the antikinks $\bar{\phi}_{k_i}(z)$ as \bar{k}_i .

4.2 Multi-kink Φ_K in the $\alpha > 0$ non-degenerate regime

In this section we analyze the properties of the Φ_K multi-kink that emerges in the $\alpha > 0$ phase. The minima v_i are no longer localized at multiples of 2π , however the topological

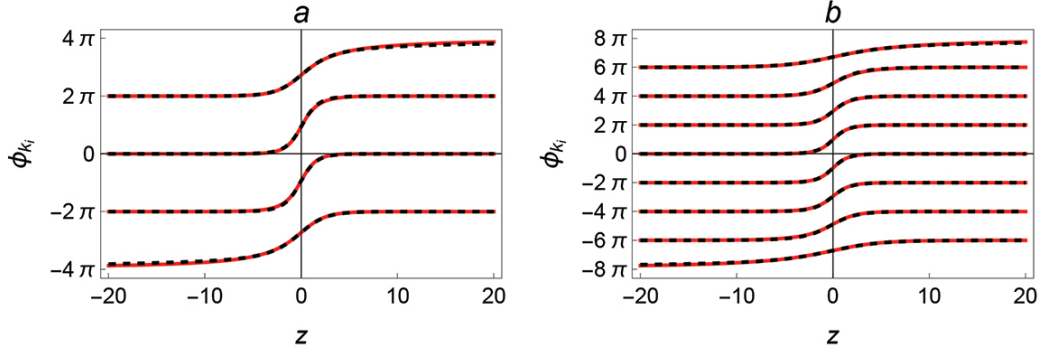


Figure 2. Kink field configurations $\phi_{k_i}(z)$ obtained from the numerical solution of Eq.(4.7) (continuous-red lines) and the analytical Eq.(4.8) (dashed-black lines); for the (a) $n = 4$ and (b) $n = 8$ cases.

charge Q_n is easily calculated because the values at the absolute minima $v_{\pm n/2} = \pm n\pi$ are not modified, hence the multi-kink interpolates between $\phi_{z \rightarrow -\infty} = v_{-n/2}$ to $\phi_{z \rightarrow \infty} = v_{n/2}$ leading to $Q_n = \frac{1}{2\pi}(v_{n/2} - v_{-n/2}) = n$, that it is the sum of the topological charges of the n subkinks $Q_n = \sum_i q_{k_i} = n$.

4.2.1 Multi-kink mass $M_{K(n,\alpha)}$

Other multilink properties can be analyzed utilizing the smooth-modulation approximation. In order to calculate the multi-kink mass $M_{K(n,\alpha)}$ we split it into the sum of the internal kink masses $M_{K(n,0)}$ and the α binding interaction energy ΔV_K , identified with the first and second terms of the following expression

$$M_{K(n,\alpha)} = \int_{-n\pi}^{n\pi} \sqrt{2V_{n,0}(\phi)} d\phi + \int_{-n\pi}^{n\pi} \left(\sqrt{2V_{n,\alpha}(\phi)} - \sqrt{2V_{n,0}(\phi)} \right) d\phi. \quad (4.11)$$

The first term is the sum of the internal kink masses M_{k_i} . Using the results in Eq.(4.6), it follows that

$$M_{K(n,0)} = \sum_{i=-\frac{n}{2}}^{\frac{n}{2}} M_{k_i} = \frac{8n^2}{n^2 - 1} \cot \frac{\pi}{2n}. \quad (4.12)$$

In order to estimate ΔV_K , the $\phi \in \{-n\pi, n\pi\}$ integration domain is split into the n intervals $\phi \in \{v_i, v_{i+1}\}$, and in each of these intervals the smooth-modulation approximation is implemented considering $1 + \cos(\frac{\phi}{n}) \approx 1 + \cos(\frac{v_i + v_{i+1}}{2n})$, hence ΔV_K can be computed as follows

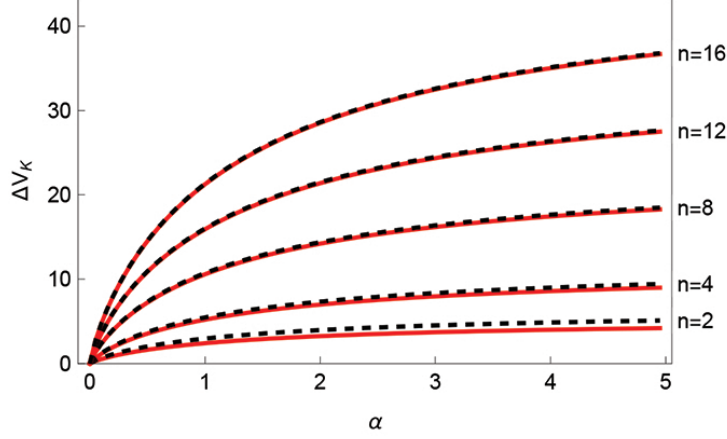


Figure 3. (a) Binding energy ΔV_K of the K^n multi-kink as a function of α , obtained from the numerical integration of the second term of Eq.(4.11) (continuous-red lines) and the analytical expression in Eq.(4.13) (dashed-black lines) for several values of n .

$$\begin{aligned}
\Delta V_K &\approx \sqrt{8} \sum_{i=0}^{\frac{n}{2}-1} \cos\left(\frac{(2i+1)\pi}{2n}\right) \int_{2i\pi}^{2(i+1)\pi} \left(\sqrt{\frac{1+\alpha-\cos\phi}{1+\frac{\alpha}{2}}} - \sqrt{1-\cos\phi} \right) d\phi \quad (4.13) \\
&= \sum_{i=0}^{\frac{n}{2}-1} \cos\left(\frac{(2i+1)\pi}{2n}\right) \left(\sqrt{32} \sqrt{\frac{\alpha}{1+\frac{\alpha}{2}}} \left(E\left[\left(i+1\right)\pi, -\frac{2}{\alpha}\right] - E\left[i\pi, -\frac{2}{\alpha}\right] \right) - 16 \right) \\
&= \left(\sqrt{\frac{32\alpha}{1+\frac{\alpha}{2}}} E\left[-\frac{2}{\alpha}\right] - 8 \right) \csc\left(\frac{\pi}{2n}\right).
\end{aligned}$$

Half of the previous integrals are given in terms of the elliptic integral of the second kind $E\left[i\pi, -\frac{2}{\alpha}\right] = 2i E\left[-\frac{2}{\alpha}\right]$, evaluated at an argument that reduces it to the corresponding complete functions, allowing us to explicitly evaluate the sum leading to the final expression given in Eq.(4.13). Adding up $M_{K(n,\alpha)}$ and ΔV_K gives the total multi-kink mass as

$$M_{K(n,\alpha)} = \left[\frac{8n^2}{n^2-1} \cos\left(\frac{\pi}{2n}\right) + \sqrt{\frac{32\alpha}{1+\frac{\alpha}{2}}} E\left[-\frac{2}{\alpha}\right] - 8 \right] \csc\left(\frac{\pi}{2n}\right). \quad (4.14)$$

The multi-kink mass includes the sum of the subkink masses $M_{K(n,0)}$, that is exactly calculated in Eq.(4.12), and the interaction energy ΔV_K that binds the n internal kinks as estimated in Eq.(4.13). Fig.(3) compares the plots obtained by the numerical integration of the second term in Eq.(4.11) and the analytical results for ΔV_K in Eq.(4.13) as a function of α . Except for $n=2$, the approximation works remarkably well throughout the range of α values.

Using the expansion $\sqrt{\frac{32\alpha}{1+\alpha}} E\left[-\frac{2}{\alpha}\right] - 8 \approx \alpha (\log \frac{32}{\alpha} - 1)$ for $\alpha \ll 1$, the limit of Eq.(4.14) yields

$$M_{K(n,\alpha)} \approx \left[\frac{8n^2}{n^2-1} \cos\left(\frac{\pi}{2n}\right) + \alpha \log\left[\frac{12}{\alpha}\right] \right] \csc\left(\frac{\pi}{2n}\right). \quad (4.15)$$

This expression is in agreement with the result obtained using the thin-wall approximation Eq.(3.9).

4.2.2 Multi-kink profile $\Phi_K^n(z)$ and size σ_K

Although the mass and other properties of the soliton solutions are well defined for all positive values of α , its multi-kink structure only becomes evident for $0 < \alpha < \alpha_1$. In this case the internal k_i and k_{i+1} kinks are well separated by a large $\xi_{i+1} - \xi_i$ distance that can be calculated from Eq.(3.6). Recalling that in each region $\phi \in \{\omega_{i-1}, \omega_i\}$, the $1 + \cos(\frac{\phi}{n})$ term varies slowly, hence it can be approximated as $1 + \cos(\frac{v_i}{n}) = 2m_i^2$, by integrating the resulting expression we find

$$\xi_{i+1} - \xi_i \approx \frac{1}{2m_i} \int_{\omega_i}^{\omega_{i+1}} \sqrt{\frac{1 + \frac{\alpha}{2}}{\frac{\alpha}{2} + \sin^2 \frac{\phi}{2}}} d\phi = \frac{1}{m_i} \sqrt{\frac{2(1 + \frac{\alpha}{2})}{\alpha}} \left(F \left[\frac{\omega_{i+1}}{2}, -\frac{2}{\alpha} \right] - F \left[\frac{\omega_i}{2}, -\frac{2}{\alpha} \right] \right), \quad (4.16)$$

where $F[\phi, k]$ is the elliptic integral function of the first kind. The expression can be reduced approximating $\omega_i \approx (2i - 1)\pi$, and using the property $F \left[\frac{2i+1}{2}\pi, -\frac{2}{\alpha} \right] = (2i + 1)K \left[-\frac{2}{\alpha} \right]$, with $K \left[-\frac{2}{\alpha} \right]$ being the complete elliptic integral function of the first kind, then Eq.(4.16) becomes

$$\xi_{i+1} - \xi_i \approx \frac{2}{m_i} \sqrt{\frac{2(1 + \frac{\alpha}{2})}{\alpha}} K \left[-\frac{2}{\alpha} \right] \approx \frac{1}{m_i} \log \left[\frac{32}{\alpha} \right]. \quad (4.17)$$

Here the last result applies in the $\alpha \ll 1$ limit, and clearly it is in agreement with the thin-wall approximation result Eq.(3.8). This result allow us to estimate the condition required to have a well defined multi-kink structure, without overlapping between its internal kinks. Considering the expression for $\phi_{k_i}(z)$ in Eq.(4.8), the width σ_{k_i} of the energy distribution of the k_i kink is estimated as $\sigma_{k_i} = \frac{8}{m_{i-1} + m_i}$. Hence demanding that the $k_i - k_{i+1}$ separation is larger than σ_{k_i} , and considering $m_{i-1} \approx m_i$, leads to the condition

$$\alpha < \alpha_1 \approx \frac{32}{\exp(4)} = 0.6. \quad (4.18)$$

Notice that the previous condition is independent of the value of n .

The previous results allow us to estimate the $\Phi_K(z)$ profile, assuming that it is written as an ansatz that adds the subkinks fields $\phi_{k_i}(z)$ in Eq.(4.8), separated by distances given in Eq.(4.16). Hence $\Phi_K(z)$ takes the following form

$$\Phi_K^n(z) = \sum_{i=1}^{\frac{n}{2}} (\phi_{k_i}(z - X_i) + \phi_{k_{-i}}(z + X_i)), \quad (4.19)$$

where the internal kinks are centered at the positions

$$X_i = \sum_{j=1}^i \left(1 - \frac{1}{2} \delta_{j,1} \right) (\xi_j - \xi_{j-1}), \quad (4.20)$$

with $\xi_0 \equiv \xi_{-1}$. The multi-kink $\Phi_K(z)$ is centered at $z = 0$. Fig.(4) compares the $\Phi_K(z)$ profile obtained from the numerical solution of the exact Bogomol'nyi Eq.(2.6) for the

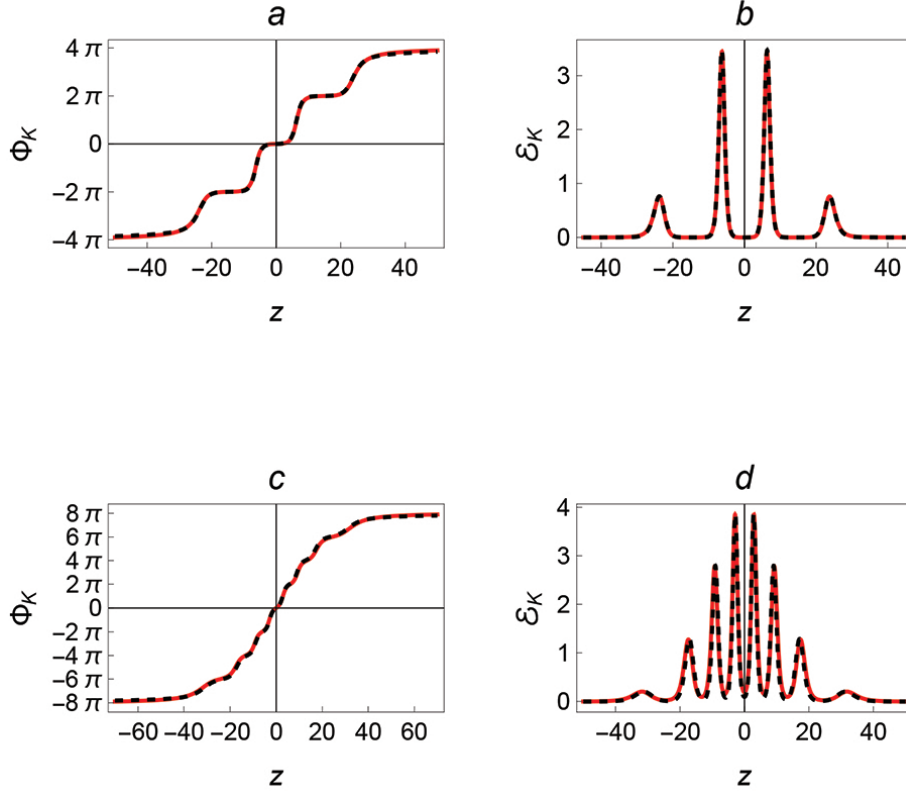


Figure 4. (a) and (c) multi-kinks $\Phi_K^n(z)$ obtained from the numerical solution of Eq.(2.6) for the potential $V_{n,\alpha}(\phi)$ in Eq.(4.1) (continuous-red lines) and the analytical ansatz Eq.(4.19) (dashed-black lines).(b) and (d) their corresponding energy density distributions. The parameters values are: $n = 4$, $\alpha = 0.0001$ for the (a) and (b) figures and $n = 8$, $\alpha = 0.1$ in the (c) and (d) cases.

potential in Eq.(4.1) with the approximated ansatz in Eq.(4.19). We observe that the approximation shows an excellent agreement with numerical calculations, improving as α decreases and n increases. The corresponding plot for the distribution of the energy density clearly displays the n localized bumps of energy associated with each of the n subkinks. For the purpose of the upcoming discussion, a multi-kink will be indistinctly denoted as Φ_K^n or K^n . We have just concluded that K^n is made up of n subkinks, hence $K^n \sim \{k_{-\frac{n}{2}}, k_{-\frac{n}{2}+1}, \dots, k_{\frac{n}{2}}\}$.

It is reasonable to assume that the size of a subkink k_i is given by the width of its energy density distribution $\sigma_{k_i} \approx \frac{8}{m_i + m_{i+1}}$. However, for a multi-kink the size must encompass the n internal subkinks k_i , plus half the width of the two exterior subkinks $k_{\pm \frac{n}{2}}$, hence we define the size σ_K of the K^n multi-kink as follows

$$\sigma_K = 2 \left(X_{\frac{n}{2}} + \frac{4}{m_{\frac{n}{2}-1}} \right), \quad (4.21)$$

where according to Eq.(4.20) $X_{\frac{n}{2}}$ represents the position of the $k_{\frac{n}{2}}$ subkink, and we take

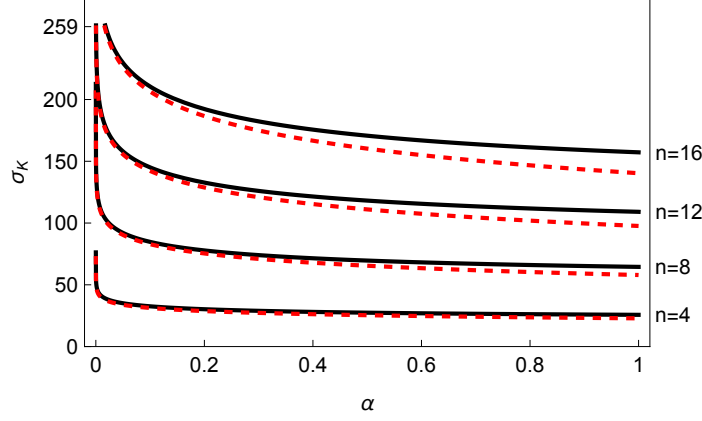


Figure 5. Size σ_K of the K^n multi-kinks as a function of α obtained from Eq.(4.21) for several values of n . The dashed lines are obtained using the approximated expression in Eq.(4.22).

into account that $m_{\frac{n}{2}}$ can be neglected. Fig.(5) displays the multi-kink size as a function of the breaking degeneracy parameter α for various values of n . The result is compared with the approximated expression

$$\sigma_K \approx \frac{2n}{\pi} \left[\left(\log\left(\frac{2n}{\pi}\right) + \frac{1}{2} \right) \log\left(\frac{32}{\alpha}\right) + 4 \right], \quad (4.22)$$

that is worked out considering $\alpha \ll 1$, $n \gg 1$ and using the approximated result $\sum_{j=1}^{\frac{n}{2}-1} \frac{1}{\cos(j\pi/n)} \approx \frac{n}{\pi} \left[\log\left(\frac{2n}{\pi}\right) + \frac{1}{2} \right]$ in Eqs.(4.17,4.20). Therefore we conclude that σ_K scales as $\sigma_K \sim \frac{2n}{\pi} \log(n) \log(\frac{1}{\alpha})$ as n grows and α decreases.

4.3 Multi-kink collisions

We now analyze the collisions between two multi-kinks, the dynamics of which are studied solving the field time dependent equation of motion Eq.(2.4) with the method of finite differences. We use a temporal grid with time steps $\tau \approx 0.12$, and for the spatial grid we consider a lattice spacing $h \approx 0.41$ with 12000 points on the total space region $z \in \{-2500, 2500\}$, with boundaries that are far enough, to ensure that they do not affect the numerical solutions. The initial multi-kink solutions are numerically determined using a fourth-order Runge-Kutta scheme. We consider two multi-kinks with an initial large separation $2L$, approaching each other with initial velocities $\pm v_{in}$. In the examples that follow we look at $n = 4$ multi-kinks, size of which is limited as $\sigma \leq 50$, according to the results in Fig. (5). In all the examples we select $L = 200$ to ensure a negligible initial overlapping of the original multi-kinks, with the corresponding improvement of the accuracy of the initial conditions. The notation $K\{v_i, v_i + 2n\pi\}$ will be used to highlight the vacuum field region in which the mutikink is defined

We first consider the collision between two $n = 4$ contiguous multi-kinks: $K\{-4\pi, 4\pi\}$ and $K\{4\pi, 12\pi\}$. Conservation of the topological charge $Q_{2 \times 4} = 8$ guarantees that the field configuration always interpolate between the asymptotic values $\phi \rightarrow -4\pi$, as $z \rightarrow -\infty$ and

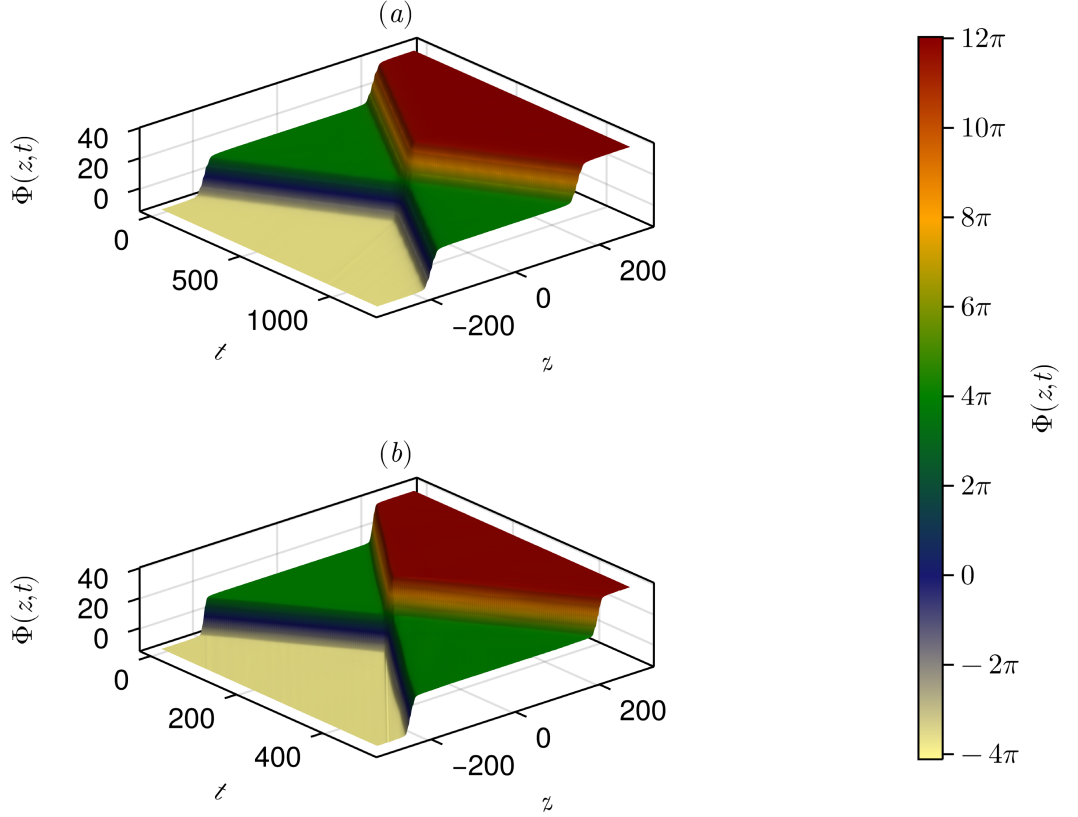


Figure 6. Space-time picture for the collision of two $n = 4$ contiguous multi-kinks $K\{-4\pi, 4\pi\}_{v_{in}} + K\{4\pi, 12\pi\}_{-v_{in}} \rightarrow K\{-4\pi, 4\pi\}_{-v_{fi}} + K\{4\pi, 12\pi\}_{v_{fi}}$. The initial velocities are: (a) $v_{in} = 0.2$ and (b) $v_{in} = 0.9$, the other parameters are selected as $L = 200$ and $\alpha = 0.05$.

$\phi \rightarrow 12\pi$, as $z \rightarrow \infty$, respectively. It is noteworthy to observe that the internal multi-kink structure is preserved by the collision for a wide range of speed values v_{in} . This is clearly shown in Figure (6) where the field configuration for the $\Phi_K^4 - \Phi_K^4$ collision is displayed when (a) $v_{in} = 0.2$ and (b) $v_{in} = 0.9$. After the multi-kinks bounce back, the initial field configuration is asymptotically recovered, with the two multi-kinks moving away with a final velocity v_{fi} . This collision is represented as $K\{-4\pi, 4\pi\}_{v_{in}} + K\{4\pi, 12\pi\}_{-v_{in}} \Rightarrow K\{-4\pi, 4\pi\}_{-v_{fi}} + K\{4\pi, 12\pi\}_{v_{fi}}$. The result is reminiscent of the sine-Gordon model, where an exact 2-solitons solution is known, in which the original solitons bounce back in an elastic collision keeping the same shape and amplitudes, the only effect being a phase shift of the original solitons. The difference is that in our example the collision is inelastic, giving rise to oscillatory excitations of the internal kinks and also some radiation energy loss. However, these effects remain small, which allows the internal multi-kink structure to be preserved by the collision.

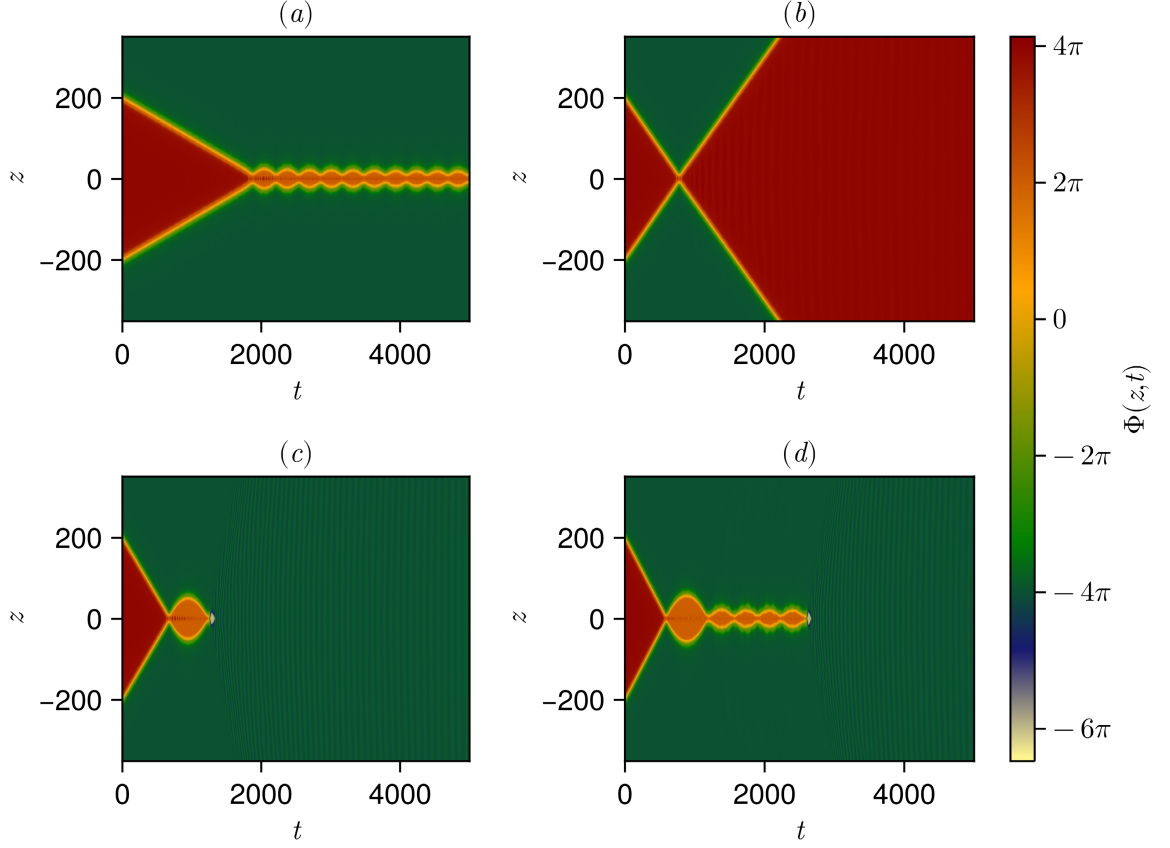


Figure 7. Space-time contour plots of the $K^4 - \bar{K}^4$ collisions with various initial velocities: (a) $v_{in} = 0.1$, (b) $v_{in} = 0.25$, (c) $v_{in} = 0.29$, and (d) $v_{in} = 0.332$. In all cases $L = 200$, $n = 4$ and $\alpha = 0.05$.

Then we study the collision of a $K\{-4\pi, 4\pi\}$ multi-kink with its corresponding $\bar{K}\{4\pi, -4\pi\}$ anti-multi-kink. In this case, the topological charge cancels and three possible outcomes of the collision are observed:

(i) The formation of a long-lived breather with internal structure, Fig. (7(a)). The plot suggests that this spatially localized and periodic in time configuration results from the fusion of the nearest $k_2 - \bar{k}_{-2}$ subkinks into a bion that oscillates around the $v = 2\pi$ false vacuum; in turn the bion remains linked to the rest of the K^4 or \bar{K}^4 parents by the binding force given in Eq.(3.7). The internal structure of the breather can be clearly identified in Figure (8), displaying a space-time three dimensional plot for the field and some snapshots of the breather at various times.

(ii) The $K^4 - \bar{K}^4$ annihilation, Figs. (7(c),(d)), where the field decays into the $v_i = -4\pi$ vacuum. The solitons bounce back repeatedly, radiating energy in every approach until not enough energy is left to produce a new rebound, leading to a rapid sequential annihilation

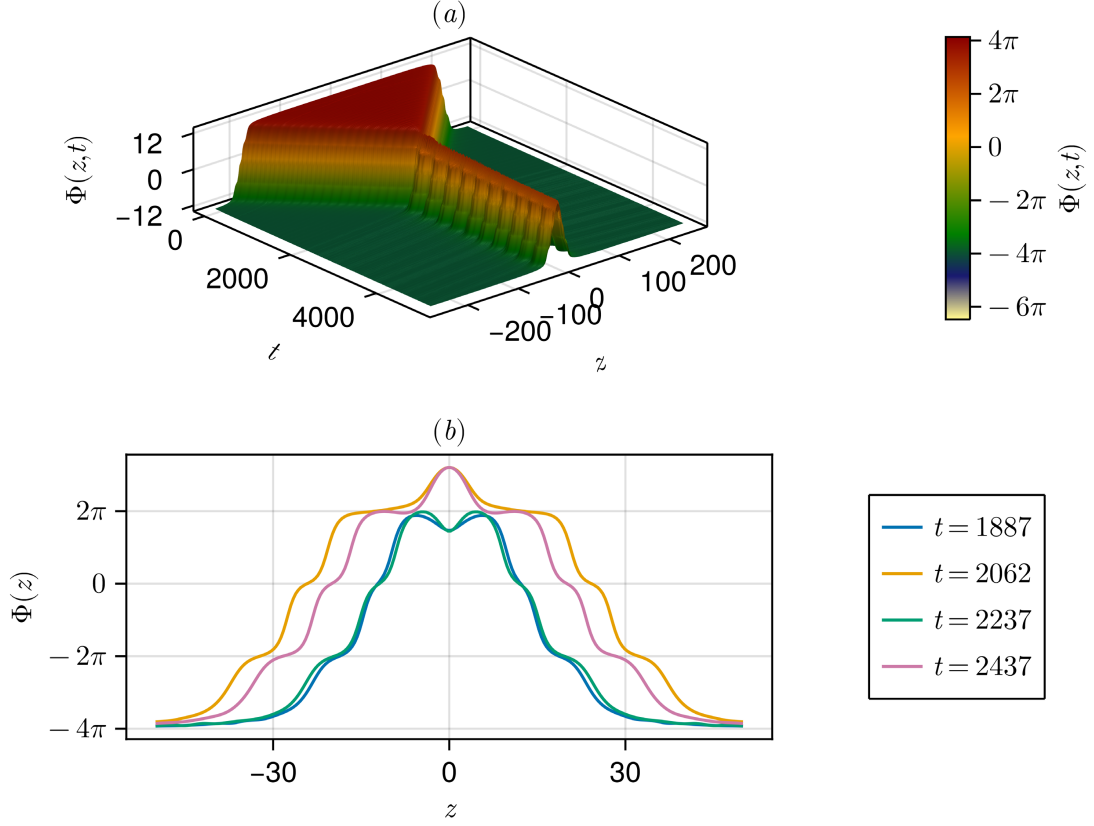


Figure 8. (a) Three dimensional plot for the $K^4 - \bar{K}^4$ collision leading to the formation of a compound breather. (b) Snapshots of the breather at various times. The parameters values are $\alpha = 0.05$, $n = 4$, $L = 200$ and $v_{in} = 0.1$.

of the internal components of K^4 with those of \bar{K}^4 , and leaving a pattern of field space-time ripples around the $v_i = -4\pi$ vacuum. These effects can be visualized in Figure (9) presenting a three dimensional plot of the field and energy density distribution evolution.

(iii) Finally, the $K\{-4\pi, 4\pi\}_{v_{in}} + \bar{K}\{4\pi, -4\pi\}_{-v_{in}} \implies K\{-4\pi, 4\pi\}_{-v_{fi}} + \bar{K}\{4\pi, -4\pi\}_{v_{fi}}$ dispersion processes in which the original solitons escape to infinity after the first bounce with a final velocity v_{fi} , Fig. (7(b)). Contrary to the well known phenomena observed in the ϕ^4 and ϕ^6 models [9, 10, 23–25, 41], in the present work we could not find multi-bounce dispersion processes. Apparently, the energy loss in each rebound inevitably leads to the annihilation of the field.

The previous described phenomena can be conveniently organized in a two dimensional $\alpha - v_{in}$ contour plot in which the different color regions are associated to the field value $\Phi_{K\bar{K}}(0, T)$ evaluated at the central collision position $z = 0$ and at large asymptotic time T , Fig. (10). An interesting chaotic behavior can be identified. We refer to the collisions

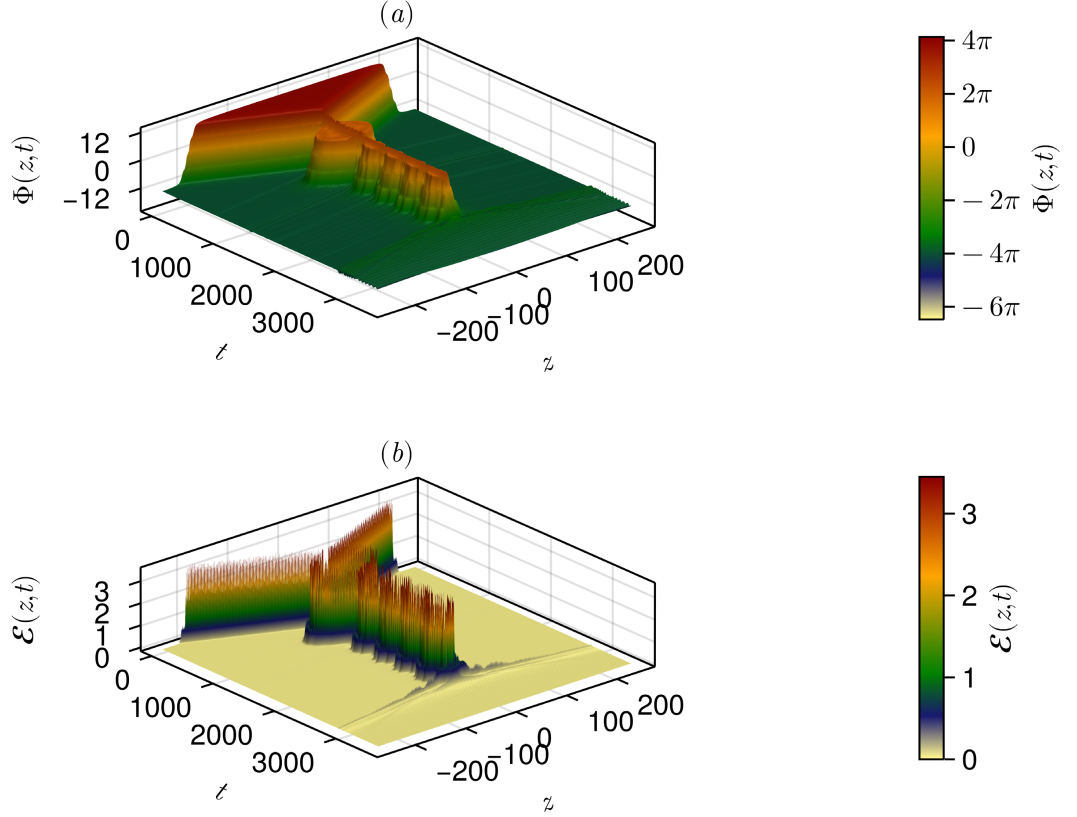


Figure 9. Three dimensional plots for the $K^4 - \bar{K}^4$ collision leading to the field annihilation after two bounces. The parameters selection is $\alpha = 0.05$, $n = 4$, $L = 200$ and $v_{in} = 0.332$.

outcomes in three α regions:

(a) The small $0.01 \leq \alpha \leq 0.1$ region. Considering small initial velocities limited as $v_{in} < 0.05$ we mainly identify breather formation. The intermediate zone $0.05 < v_{in} < 0.15$ is characterized by the increasing apparition of inelastic dispersion island. This is followed by the $0.15 < v_{in}$ zone where we identify the formation of large dispersion spikes and also some scarce annihilation islands.

(b) The intermediate $0.1 \leq \alpha \leq 0.15$ region where breathers and annihilations dominate, and very few dispersion zones are left.

(c) Lastly, as the value of α increases above 0.15 both the number of breathers and dispersion regions abruptly decrease, until the annihilation processes completely dominate. The plot shows that there is a $\alpha_c \approx 0.17$ threshold value, so for any $\alpha > \alpha_c$ annihilation is the only possible collision outcome, independently of the v_{in} value.

Fig. (11a) displays the time evolution of the field central value $\Phi_{K\bar{K}}(0, t)$ as a function of the initial velocity v_{in} for $\alpha = 0.065$. We observe a series of intercalated windows

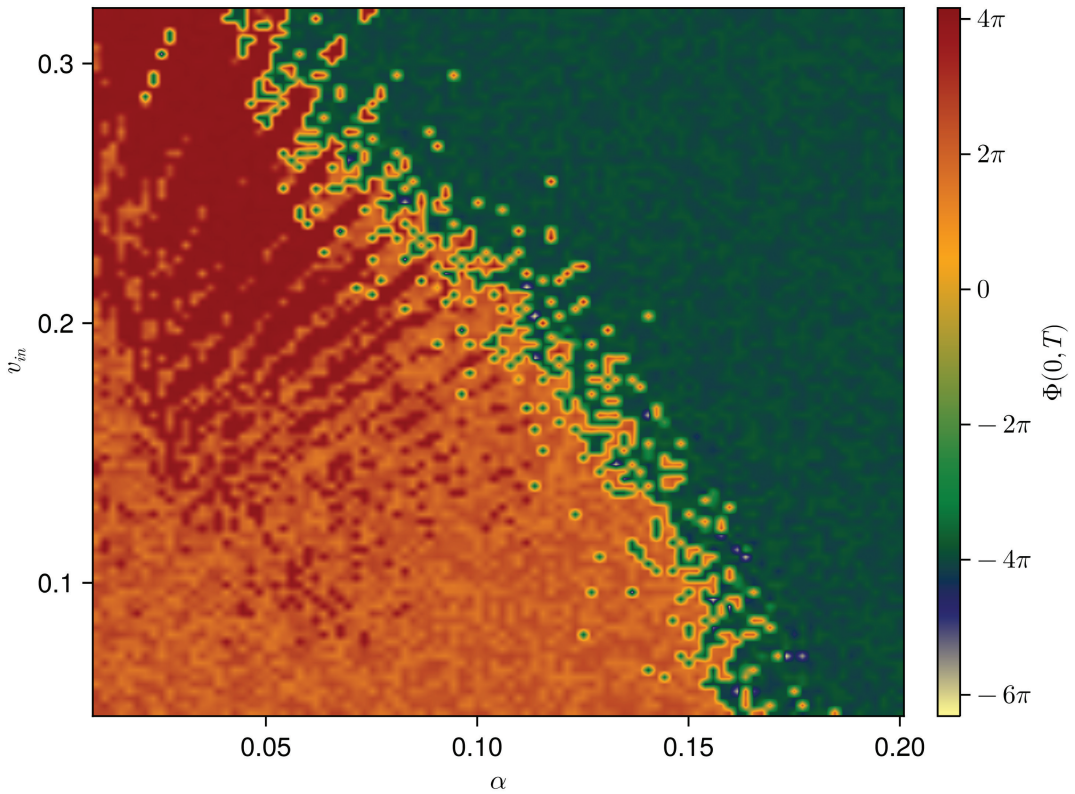


Figure 10. Asymptotic value of the total field configuration for the $K^4 - \bar{K}^4$ collision, evaluated at the centre of the collision ($z = 0$) at a large time $T \approx 3000$, as a function of the initial velocity v_{in} and the α breaking degeneracy parameter. T is measured once the initial trajectories intersect.

corresponding to annihilations and inelastic dispersions, surrounded by regions of bion formation. The three magnification images in Fig. (11b,c,d) obtained from a consecutive reduction of the v_{in} intervals show that new annihilation and dispersion windows become evident as a result of the magnification processes. This replications pattern for the windows clearly suggests a fractal behavior for the $K^4 - \bar{K}^4$ collisions.

5 Conclusions

We have shown that for generic scalar field models with multiple potential minima, the partial breaking of the vacuum degeneracy provides a mechanism for the appearance of multi-kinks. This will be the case whenever some false vacuum states appear between two true vacuums. The demonstration is carried out using the analogy “static soliton profile versus motion of a point particle”, and the thin-wall approximation. The formulation of the dynamical Bogomol’nyi relation Eq.(3.4), is of particular relevances, providing an explicit

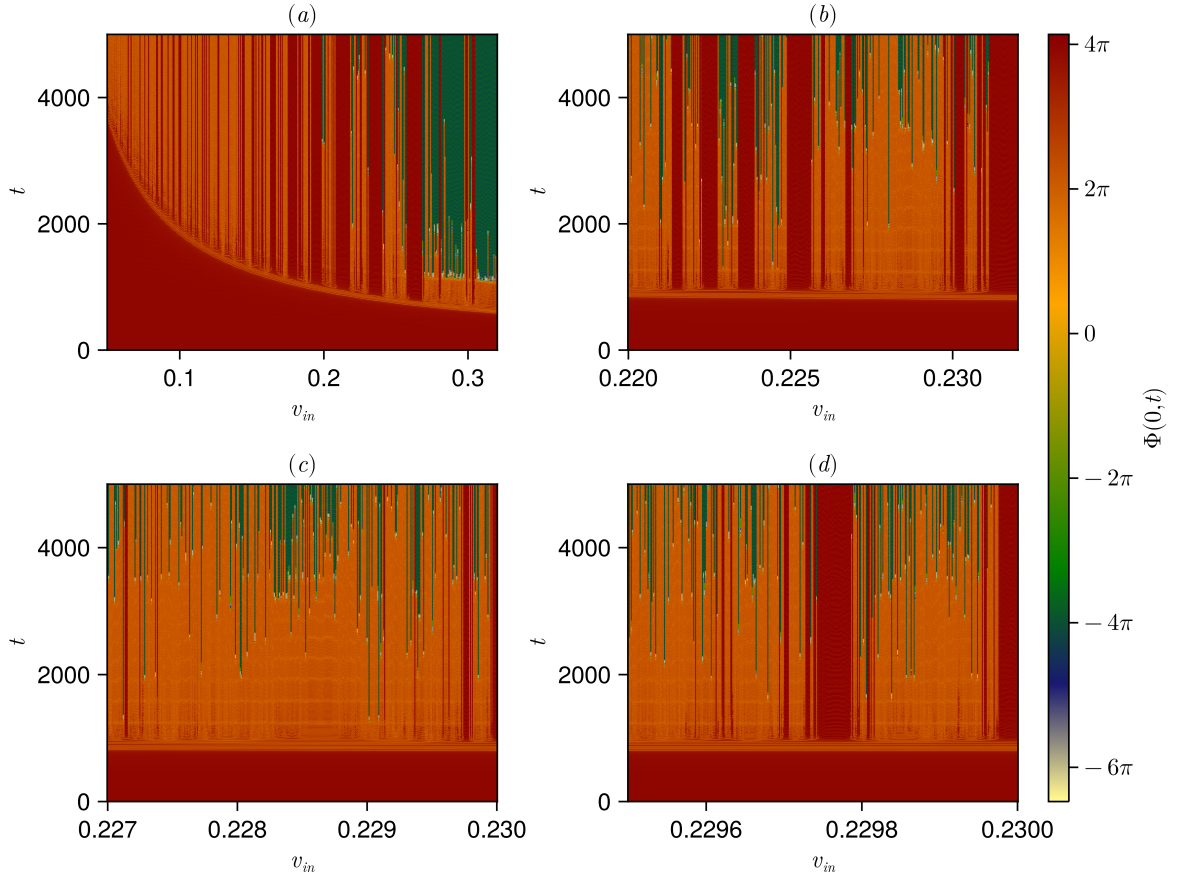


Figure 11. (a) Time evolution of the field central value $\Phi_{K\bar{K}}(0, t)$ as a function of the initial velocity v_{in} for $\alpha = 0.065$, $v_{in} \in \{0.01, 0.3\}$. Three magnification plots for the regions: (b) $v_{in} \in \{0.22, 0.235\}$, (c) $v_{in} \in \{0.227, 0.23\}$, (d) $v_{in} \in \{0.2295, 0.23\}$

expression for the separation between contiguous subkinks Eq.(3.8), which in turn enables the estimation of the total mass $M_{K(n,\alpha)}$ of the multi-kink Eq.(3.9). It is worth noting that these results are obtained even though the configuration of the field $\Phi_K(z)$ is not known. We thus observe the general validity of the following scaling results: $\xi_{i+1} - \xi_i \propto \frac{1}{m_i} \log \frac{1}{\alpha}$ for the subkink separation and $\Delta V_K \propto \alpha \log \frac{1}{\alpha}$ for the binding interaction energy of the multi-kink.

The vacuum degeneracy breaking mechanism provides a useful guide to construct scalar field models that possess multikink solutions, allowing us to propose the commensurable and non degenerate double sine-Gordon model which admits multi-kink configurations with arbitrary n internal subkinks. It was not possible to find exact analytical field solutions, but the smooth modulation approximation works remarkably well, allowing us to carry out an exhaustive analysis for multi-kinks properties. Multi-kinks obey the obvious proportionality relations $Q_n = n$ and $M_{K(n,\alpha)} \propto n$. An interesting result is obtained for the multi-kink size

that scales as $\sigma_K \sim \frac{2n}{\pi} \log(n) \log(\frac{1}{\alpha})$ as n increases and α decreases, where the higher to linear n growth follows because the subkinks separations increase as they move away from the center of the multi-kink.

The multi-kinks collision within the proposed model opens a wide and interesting perspective for the study of novel collective phenomena, which we started exploring for the $n = 4$ case. Although the subkinks are weakly bound in the $\alpha \leq \alpha_1$ region of interest, the results obtained proved that the multi-kink structure is robust. This is the case for the $K^4 - K^4$ collision, where we found that the multi-kinks emerge from the collision recovering their internal structure for a wide range of values of the initial incident velocity. On the other hand, for the $K^4 - \bar{K}^4$ collisions we observed the production of long-lived breathers with an internal structure which reflects the initial composition of the multi-kinks. Similarly to the results for the ϕ^4 and ϕ^6 studies, we identified repeated bounces of the multi-kinks. However, in clear contrast to these previous cases, here the outcome of the processes is always a $K^4 - \bar{K}^4$ annihilation. The inelastic dispersion, in which the incident multi-kinks bounce back separating to infinity is indeed present, but we find a complete suppression of all multi-bounce dispersion windows for the K^4 and \bar{K}^4 collisions. The different regions for the occurrence of these processes can be identified in a $\alpha - v_{in}$ contour plot that presents a chaotic behavior, with a similar structure to the one obtained in previous studies [35, 41], but with the specific differences mentioned above. In particular, we found a threshold value $\alpha_c \approx 0.17$ above which annihilation is the only possible collision outcome, independently of the v_{in} value.

We consider that the results of this work offer an interesting scenario that deserve further analysis and may be relevant in the study of the emergence of coherent structures in physical systems [17, 42].

References

- [1] R. Rajaraman, *Solitons and instantons. An introduction to solitons and instantons in quantum field theory*, North-Holland, Netherlands (1982).
- [2] S. Coleman, *Classical Lumps and Their Quantum Descendants*, Springer US, Boston, MA (1977), [10.1007/978-1-4613-4208-3-11](#).
- [3] N. Manton and P. Sutcliffe, *Topological Solitons.*, Cambridge Monographs on Mathematical Physics, United Kingdom (2004).
- [4] T. Vachaspati, *Kinks and Domain Walls: An Introduction to Classical and Quantum Solitons*, Cambridge University Press (2006), [10.1017/CBO9780511535192](#).
- [5] E. Weinberg, *Classical Solutions in Quantum Field Theory: Solitons and Instantons in High Energy Physics.*, Cambridge Monographs on Mathematical Physics, United Kingdom (2012).
- [6] R.F. Dashen, B. Hasslacher and A. Neveu, *Nonperturbative methods and extended-hadron models in field theory. ii. two-dimensional models and extended hadrons*, [Phys. Rev. D](#) **10** (1974) 4130.
- [7] P.G. Kevrekidis and J. Cuevas-Maraver, *Historical A Dynamical Perspective on the ϕ^4 Model: Past, Present and Future*, Springer Cham, Switzerland (2019).

- [8] V. Makhankov, *Dynamics of classical solitons in non-integrable systems*, *Physics Reports* **35** (1978) 1.
- [9] M. Moshir, *Soliton-antisoliton scattering and capture in the ϕ^4 theory*, *Nuclear Physics B* **185** (1981) 318.
- [10] D.K. Campbell, J.F. Schonfeld and C.A. Wingate, *Resonance structure in kink-antikink interactions in ϕ^4 theory*, *Physica D: Nonlinear Phenomena* **9** (1983) 1.
- [11] P. Anninos, S. Oliveira and R.A. Matzner, *Fractal structure in the scalar $\lambda(\phi^2 - 1)^2$ theory*, *Phys. Rev. D* **44** (1991) 1147.
- [12] F. Simas, A. Gomez, K. Nobrega and J. Oliveira, *Suppression of two-bounce windows in kink-antikink collisions.*, *Journal of High Energy Physics* **2016** (2016) 1.
- [13] T. Sugiyama, *Kink-antikink collisions in the two-dimensional ϕ^4 model*, *Prog Theor Phys* **61** (1979) 1550.
- [14] I. Takyi and H. Weigel, *Collective coordinates in one-dimensional soliton models revisited*, *Phys. Rev. D* **94** (2016) 085008.
- [15] N.S. Manton, K. Oleś, T. Romańczukiewicz and A. Wereszczyński, *Kink moduli spaces: Collective coordinates reconsidered*, *Phys. Rev. D* **103** (2021) 025024.
- [16] N.S. Manton, K. Oleś, T. Romańczukiewicz and A. Wereszczyński, *Collective coordinate model of kink-antikink collisions in ϕ^4 theory*, *Phys. Rev. Lett.* **127** (2021) 071601.
- [17] A. Scott, *Nonlinear Science: Emergence and Dynamics of Coherent Structures*, Oxford University Press, United Kingdom (2003).
- [18] J. Cuevas-Maraver, P.G. Kevrekidis and F. Williams, *The sine-Gordon Model and its Applications: From Pendula and Josephson Junctions to Gravity and High-Energy Physics*, Springer Cham, Switzerland (2014).
- [19] M.J. Ablowitz, D.J. Kaup, A.C. Newell and H. Segur, *Method for solving the sine-gordon equation*, *Phys. Rev. Lett.* **30** (1973) 1262.
- [20] V. Zakharov, L. Takhtajan and L. Faddev, *Complete description of solutions of the the sine-gordon equation*, *Doklady AN SSSR* **219** (1973) 1334.
- [21] D.K. Campbell, M. Peyrard and P. Sodano, *Kink-antkink interactions in the double sine-gordon equation*, *Physica D: Nonlinear Phenomena* **19** (1986) 165.
- [22] P. Grinevich and S. Novikov, *Topological charge of the real periodic finite-gap sine-gordon solution*, *Commun. Pure Appl. Math.* **56** (2003) 956.
- [23] P. Dorey, K. Mersh, T. Romanczukiewicz and Y. Shnir, *Kink-antikink collisions in the ϕ^6 model*, *Phys. Rev. Lett.* **107** (2011) 091602.
- [24] A. Demirkaya, R. Decker, P.G. Kevrekidis, I.C. Christov and A. Saxena, *Kink dynamics in a parametric ϕ^6 system: a model with controllably many internal modes*, *Journal of High Energy Physics* **2017** (2017) 1.
- [25] A. Moradi Marjaneh, V.A. Gani, D. Saadatmand, S.V. Dmitriev and K. Javidan, *Multi-kink collisions in the ϕ^6 model*, *Journal of High Energy Physics* **2017** (2017) 28.
- [26] V.A. Gani, A.M. Marjaneh and P.A. Blinov, *Explicit kinks in higher-order field theories*, *Phys. Rev. D* **101** (2020) 125017.

- [27] A. Khare, I.C. Christov and A. Saxena, *Successive phase transitions and kink solutions in ϕ^8 , ϕ^{10} and ϕ^{12} field theories*, *Phys. Rev. E* **90** (2014) 023208.
- [28] N.S. Manton, *Forces between kinks and antikinks with long-range tails*, *Journal of Physics A: Mathematical and Theoretical* **52** (2019) 065401.
- [29] I.C. Christov, R.J. Decker, A. Demirkaya, V.A. Gani, P.G. Kevrekidis, A. Khare et al., *Kink-kink and kink-antikink interactions with long-range tails*, *Phys. Rev. Lett.* **122** (2019) 171601.
- [30] E. Belendryasova and V.A. Gani, *Scattering of the ϕ^8 kinks with power-law asymptotics*, *Communications in Nonlinear Science and Numerical Simulation* **67** (2019) 414.
- [31] I.C. Christov, R.J. Decker, A. Demirkaya, V.A. Gani, P. Kevrekidis and A. Saxena, *Kink-antikink collisions and multi-bounce resonance windows in higher-order field theories*, *Communications in Nonlinear Science and Numerical Simulation* **97** (2021) 105748.
- [32] N.H. Christ and T.D. Lee, *Quantum expansion of soliton solutions*, *Phys. Rev. D* **12** (1975) 1606.
- [33] d.S.A. de Brito G.P., *Multikink solutions and deformed defects*, *Annals of Physics* **351** (2014) 620.
- [34] J. Lozano-Mayo and M. Torres-Labansat, *Kink solutions in a generalized scalar ϕ_g^4 field model*, *Journal of Physics Communications* **5** (2021) 025004.
- [35] P. Dorey, A. Gorina, T. Romańczukiewicz and Y. Shnir, *Collisions of weakly-bound kinks in the christ-lee model*, *Journal of High Energy Physics* **2023** (2023) 1.
- [36] S. Coleman, *Fate of the false vacuum: Semiclassical theory*, *Phys. Rev. D* **15** (1977) 2929.
- [37] E. Bogomolny, *The stability of classical solutions*, *Sov. J. Nucl. Phys.* **24** (1976) 449.
- [38] L.J. Boya and J. Casahorran, *General scalar bidimensional models including kinks*, *Annals of Physics* **196** (1989) 361 .
- [39] N.S. Manton, *Integration theory for kinks and sphalerons in one dimension*, *J. Phys. A* **57** (2023) 025202.
- [40] A. Alonso-Izquierdo, S. Navarro-Obregón, K. Oles, J. Queiruga, T. Romanczukiewicz and A. Wereszczynski, *Semi-bogomol'nyi-prasad-sommerfield sphaleron and its dynamics*, *Phys. Rev. E* **108** (2023) 064208.
- [41] P. Dorey, A. Gorina, I. Perapechka, T. Romańczukiewicz and Y. Shnir, *Resonance structures in kink-antikink collisions in a deformed sine-gordon model*, *Journal of High Energy Physics* **2021** (2021) 1.
- [42] N. Xu, J. Chen, Y.-P. Zhang and Y.-X. Liu, *Multikink brane in gauss-bonnet gravity and its stability*, *Phys. Rev. D* **107** (2023) 124011.